Astron. & Astrophys. 42, 311 – 321 (1975)

Radiative Transfer in a Strong Magnetic Field and Accreting X-ray Pulsars

M. M. Basko and R. A. Sunyaev
Space Research Institute, Academy of Sciences of the USSR, Moscow

Received January 20, 1975

Summary. When matter accretes onto a neutron star endowed with a strong magnetic field $H \gtrsim 10^{12} \div 10^{13}$ Gauss, its kinetic energy is liberated in the vicinity of the magnetic poles. The accreting protons with energy ~ 140 MeV are stopped by nuclear encounters in a layer as deep as 50 g cm^{-2}; Coulomb collisions in plasma with a strong magnetic field are insignificant.

As a result of high anisotropy in the scattering cross-section of photons by electrons in a magnetized plasma, the radiation emerging from the surface at frequencies $\nu \ll \nu_H$ has a "pencil" beam pattern and is highly polarized. The problem of radiative transfer in an atmosphere with a strong magnetic field is solved, and the results are presented in this paper. The mechanism being discussed can account also for the beamed and polarized radiation of white dwarfs having a strong magnetic field. In the framework of the theoretical model adopted, an upper limit is obtained for the luminosity of X-ray pulsars, which can greatly exceed the Eddington critical value per unit surface area. The luminosity of X-ray pulsars is limited by distortion of the beam pattern due to the scattering of emitted X-rays by the electrons of the infalling gas.

Key words: X-ray pulsars — radiative transfer — X-ray beaming mechanisms

1. Introduction

Two regularly pulsing X-ray sources are now known: Her X-1 and Cen X-3; both are in binary systems. They are believed to be rotating neutron stars endowed with a strong magnetic field. Accretion of matter flowing out of the normal component is then the energy source for X-ray emission. The magnetic field funnels the accreting material towards the magnetic poles, where the kinetic energy of free fall is converted into X-rays. But one cannot explain the pulsed emission of X-ray pulsars merely by the presence of hot spots on the surface of a rotating neutron star. The isotropically radiating hot spots cannot give such a deeply modulated pulse shape. The X-ray emission of hot spots must be beamed. On the other hand, in the presence of a strong magnetic field, the cross-sections and probabilities of elementary processes of interaction between radiation and matter depend on the angle θ between the field direction and the direction of electro-magnetic wave propagation, $\sigma \propto \sigma_0 \sin^2\theta$ (Canuto *et al.*, 1971; Lodenquai *et al.*, 1974). This means that at small angles θ one can see deep layers of the stellar atmosphere. If the energy source is localized deep enough in the atmosphere, then the radiation energy density increases with optical depth. As a result, X-rays emerging from the neighborhood of the magnetic poles of the accreting neutron star have a characteristic "pencil" beam pattern (Gnedin and Sunyaev, 1974; Daishido, 1973). Evidently, all these arguments also hold for the optical radiation of white dwarfs with a strong magnetic field.

Below, we discuss in detail the generation and diffusion of radiation in a plasma with a strong magnetic field; the calculated X-ray pulse shape is shown in Fig. 1; the spectrum and polarization of emerging X-rays are also discussed. The strength of the magnetic field which is required by our model to make the theoretical pulse shape close to that observed is $H \sim 10^{12} \div 10^{13}$ Gauss. The angular distribution of the outgoing radiation strongly depends on the ratio of photon frequency ν to the electron cyclotron frequency $\nu_H = eH/2\pi m_e c$. Of particular interest is the case $kT_e \simeq h\nu_H$. In this case, a narrow beam is formed at frequencies $\nu \ll \nu_H$, and the pulse shape is much more smooth when $\nu \gtrsim \nu_H$. Near ν_H a powerful emission gyroline should be present in the spectrum.

Other beaming mechanisms proposed so far (Gnedin and Sunyaev, 1973a; Bisnovatyi-Kogan, 1973) have invoked a thin collisionless shock near the surface of the neutron star, in which accreting gas is stopped. But the existence of such a collisionless shock in the

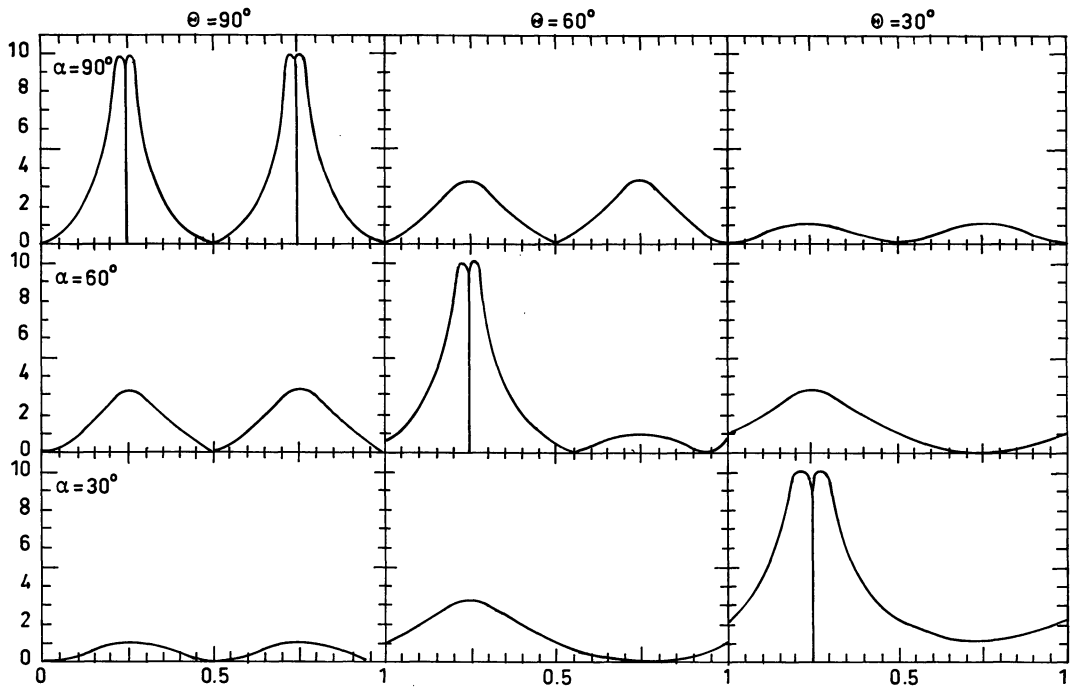

Fig. 1. The X-ray pulse profile, as calculated from the obtained beam pattern, for different values of the angle α between the spin axis of the neutron star and the magnetic dipole axis, and of the angle Θ between the spin axis and the line of sight. The abscissae are the pulse phases normalized to one complete revolution of the neutron star. The ordinates are the values of the radiative flux (in arbitrary units) as detected by distant observer

flow of particles moving along magnetic field lines is far from evident, especially in the situation under consideration where $v_H \gg v_{pl}$, $hv_H > kT_e$ and the velocity distribution of electrons is essentially one-dimensional. In the model for the radiation pattern of X-ray pulsars proposed below, the accreting gas flow is supposed to be stopped by nuclear collisions. The contribution of Coulomb collisions in a strong magnetic field is shown to be negligible.

2. Accretion Picture

2a) Flow Pattern near the Surface of the Neutron Star

Outside the Alfvén surface, where the influence of the stellar magnetic field can be neglected, the accreting matter is assumed to form a disk. The material feeding the disk flows from the normal component of the binary. At some radius R_A – the Alfvén radius – the pressure of the magnetic field of the neutron star $H^2/8\pi$ destroys the disk. We assume that in this region the transition occurs in a flow pattern from the orbital motion in the disk to a free fall onto the neutron star along its magnetic field lines, accreting plasma being "frozen" into magnetic field (Pringle and Rees, 1972; Davidson and Ostriker, 1973; Lamb *et al.*, 1973). If the rotation axis of the neutron star and the magnetic dipole axis are not aligned, the lines of constant magnetic pressure $H^2/8\pi$ in the disk plane are obviously not circles (Illarionov and Sunyaev, 1975). Consequently, the accreting matter will "freeze" into the magnetic field not along the whole of the line of constant magnetic pressure but in two opposite regions, the ones most distant from the neutron star. Owing to a low freezing rate, plasma penetrates to the magnetic field of the dipole only for a small depth, which is much less than the Alfvén radius R_A. For this reason, the gas should fall onto each magnetic pole in a long and narrow funnel (see Fig. 2). At the surface of the neutron star the cross-section of this funnel extends along the circumference of radius $a \sim 0.1R \simeq 10^5$ cm, centered at the magnetic pole (R is the radius of the neutron star). The adopted value of a agrees with the estimates for the hot-spot radius obtained earlier (Pringle and Rees, 1972; Lamb *et al.*, 1973; Baan and Treves, 1973). The width of the accretion channel is $d \ll a$. In numerical calculations, we shall use the following values for the parameters of the cross-section of the accretion column: the length $l = 2a = 2 \times 10^5$cm; the width $d = 5 \times 10^3$cm that corresponds to freezing depth $\simeq 0.1\, R_A$ at the Alfvén surface.

It should be emphasized that the angular distribution of emerging X-rays depends neither on the accretion flow pattern nor on the shape of the hot spot. The flow pattern affects only the limiting value of the X-ray luminosity, beyond which scattering by the infalling gas tends to make the hot spot emit isotropically.

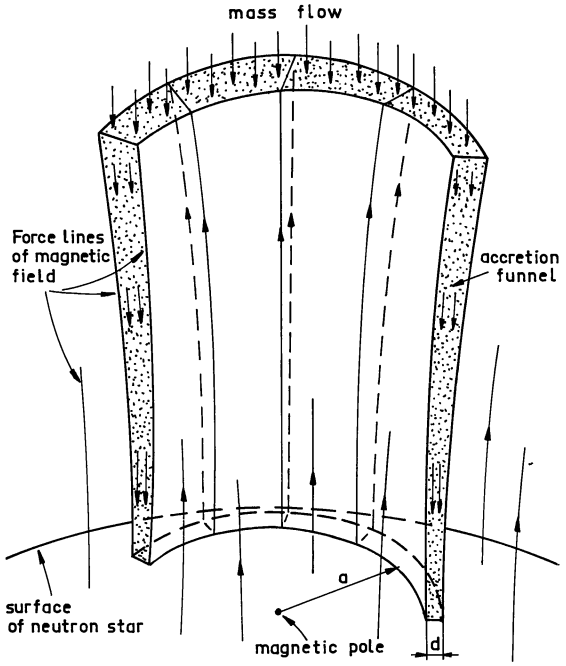

Fig. 2. The accretion funnel near the surface of the neutron star

2b) How the Infalling Matter Is Stopped

The infalling gas arrives at the surface of the neutron star with a velocity $v \simeq \frac{1}{2}c$ and an energy $E_p \simeq 140$ MeV per nucleon. It is well known that, in a non-magnetized plasma, charged particles with this energy are decelerated essentially by distant Coulomb encounters with plasma electrons, owing to transverse momentum transfer.

According to quantum theory, the energy of transverse motion of electrons in magnetic field can change only by some multiple to $h\nu_H$. If the magnetic field is sufficiently high

$$H > H_0 = \pi \frac{m_e^2 v^2 c}{he} = 5.5 \times 10^{12} \left(\frac{2v}{c}\right)^2 \text{ Gauss},$$

so that $h\nu_H > \frac{1}{2} m_e v^2$, the fast ($h\nu/2\pi e^2 \gg 1$) proton moving along the field line cannot increase the transverse energy of the electrons of the ambient plasma. Basko and Sunyaev (1975) have shown that in this case Coulomb energy losses by fast protons become negligible as compared to the nuclear encounters.

Essentially, the main processes responsible for Coulomb deceleration of the fast proton moving along a magnetic field direction at $H > H_0$ are (i) pitch-angle diffusion; and (ii) head-on collisions by which electrons are reflected from the proton in its rest frame. The first of these two mechanisms operates as follows: after a large number of scatters the proton deviates from its initial direction of motion by the angle $\theta \simeq (m_e/m_p)^{1/4}$ with a practically constant value of kinetic energy, and then rapidly gives up this energy to environmental electrons, increasing their velocity along the field lines. This qualitative picture is described by the following equation:

$$\frac{d^2 E_p^2}{dz^2} = -\left(N_e \frac{8\pi e^4 \ln \Lambda}{m_e v^2}\right)^2 \frac{m_e}{m_p}. \tag{1}$$

We recall that the equation describing the slowing down of fast protons in a field-free plasma (Landau, 1937; Fermi, 1950) is:

$$\frac{dE_p}{dz} = -N_e \frac{4\pi e^4}{m_e v^2} \ln \Lambda. \tag{2}$$

Having solved Eqs. (1) and (2), one finds that, if pitchangle diffusion only is taken into account, the Coulomb stopping distance for protons moving initially along the magnetic field lines increases in a strong field $H > H_0$ by a factor of

$$l_{H>H_0}/l_{H=0} = \left(\frac{\pi}{2}\frac{m_p}{m_e}\right)^{1/2} \simeq 54.$$

Note that this stopping distance does not depend on the magnetic field strength H.

Head-on collisions were analysed by Ventura (1973). Their contribution to the Coulomb deceleration rate can be neglected so long as $H < 10 H_0$ (at $H = H_0$ the stopping distance for this process exceeds that for pitch-angle diffusion by a factor of 2). However, it increases with magnetic field strength H and begins to dominate at $H \gtrsim 10 H_0$. As $H \to \infty$, head-on collisions become ~ 2.5 times more effective than pitch-angle diffusion.

In a more moderate magnetic field $H < H_0$ the Coulomb deceleration of protons is described by Eq. (2) where one must substitute $\ln(r_H/\lambda\!\!\!^{-})$ for the Coulomb logarithm $\ln\Lambda$ [which in our case takes the value ~ 10 (Lamb *et al.*, 1973)]. Here $r_H = (hc/\pi eH)^{1/2}$ is the radius of the lowest Landau orbit, and $\lambda\!\!\!^{-} = h/2\pi m_e v$ is the de Broglie wavelength of the electron.

Thus, in plasma having this kind of magnetic field, $H \gtrsim H_0$, the Coulomb mean free path of accreting protons is large, and they are stopped by nuclear collisions. The cross-section for nucleon-nucleon scattering is $\sigma_{pp} = 3 \times 10^{-26} \text{cm}^2$, which corresponds to the mean free path $\simeq 50 \text{g cm}^{-2}$. We note that the mean free path for Coulomb collisions exceeds the value 50g cm^{-2} so long as $H \geqslant H_0/4 = 1.4 \times 10^{12}$ Gauss. Therefore, the rate of energy release by accretion varies in the atmosphere of the neutron star as $\exp(-\tau/\tau_0)$, where $\tau = \sigma_T \int_z^\infty N_e dz$ is the optical depth for Thomson scattering, and $\tau_0 = 20$ corresponds to the mean free path 50g cm^{-2}.

The kinetic energy of accreting electrons is small compared to the energy of protons; the electron-electron collisions give a negligible contribution to the deceleration rate. The electrons will then be stopped by the electrostatic field generated by the difference in concentration of protons and electrons.

3. Elementary Processes in a Strong Magnetic Field

The magnetic field drastically reduces the cross-section of Thomson scattering and that of free-free absorption at frequencies $h\nu < h\nu_H = 11.6(H/10^{12}$ Gauss)keV (the electrons can move freely along the magnetic field lines while the transverse motion is confined to circular orbits). The electromagnetic waves propagating in the magnetized plasma have two normal modes usually called the "extraordinary wave" and the "ordinary wave". Each of these modes has its own transfer coefficient, phase velocity and polarization. Canuto *et al.* (1971) have shown that the total cross-sections for scattering by electrons in the limit $\nu \ll \nu_H$ can be approximated by the following expressions:

$$\sigma_1 = \sigma_T (\nu/\nu_H)^2 ,$$
$$\sigma_2(\theta) = \sigma_T [\sin^2\theta + (\nu/\nu_H)^2] . \tag{3}$$

Here and below the extraordinary and the ordinary waves are denoted by subscripts "1" and "2" respectively; θ is the angle with respect to the magnetic field lines at which the photon propagates before being scattered. The free-free absorption coefficients take the analogous form:

$$k_{ff}^{(1)} = k_{ff}(H=0)\,(\nu/\nu_H)^2 ,$$
$$k_{ff}^{(2)}(\theta) = k_{ff}(H=0)\,[\sin^2\theta + (\nu/\nu_H)^2] ; \tag{4}$$

these expressions can be easily derived from the well-known formula (Ginzburg and Ruhadze, 1970) for the dielectric permeability of magnetized plasma (Gnedin and Sunyaev, 1973b).

In the case of interest here, when $\nu \ll \nu_H$, we may ignore the generation and diffusion of radiation in an extraordinary wave and restrict our consideration to the ordinary wave only. The reason for this may be stated as follows:

(i) The energy of the infalling gas heats the plasma in the layer $\tau \lesssim \tau_0$. The plasma cools through Compton scattering and gives up its energy predominantly to photons of the ordinary wave (cf. the expressions (3) for cross-sections).

(ii) A substantial fraction of the ordinary wave photons is "pumped over" into the extraordinary wave in a layer as deep as $\Delta\tau^* \sim \nu_H/\nu$. To prove this, we note that the typical photon of the ordinary wave traverses diffusively the layer $\Delta\tau$ for the time interval $\sim(\Delta\tau)\,(\Delta z)/c$. The cross-section of transition from the ordinary wave to the extraordinary one by scattering is $\sigma_{12} \simeq \sigma_T(\nu/\nu_H)^2$. Then the fraction of the ordinary wave photons transformed into photons of the extraordinary wave in the layer $\Delta\tau$ is $\sim(\Delta\tau)^2(\nu/\nu_H)^2$. Since the extraordinary wave freely escapes from the atmosphere, the radiative energy density drops inwardly at $\tau > \tau_0$ (see Fig. 4). The ratio of the radiation flux carried away by the extraordinary wave to that carried away by the ordinary wave is $Q_1/Q_2 \sim \tau_0/\Delta\tau^* \sim \tau_0(\nu/\nu_H)$. More detailed calculations give $Q_1/Q_2 \lesssim 10(\nu/\nu_H)$ when $\tau_0 = 20$. Thus, our model can be applyed to the real situation so long as $\nu/\nu_H < 0.1$.

To solve the equation of radiative transfer, one needs to know not only the total cross-section but also the differential one. Taking the limit $\nu/\nu_H \to 0$ in the formulae for cross-sections obtained by Canuto *et al.* (1971), we arrive at

$$d\sigma_{22}(\theta \to \theta') = (3/8\pi)\,\sigma_T \sin^2\theta\,\sin^2\theta'\,d\Omega' ,$$
$$d\sigma_{11}(\theta \to \theta') = d\sigma_{12}(\theta \to \theta') = d\sigma_{21}(\theta \to \theta') = 0 . \tag{5}$$

Here θ' is the angle at which the photon is scattered as measured from the magnetic field lines. We note that as far as the limiting case $\nu \ll \nu_H$ is concerned, the spectrum and the angular pattern of the emergent radiation do not in fact depend on the value of magnetic field strength H.

4. Physical Parameters of the Atmosphere in Hot Spots

4a) Temperature of Hot Spots

We shall obtain a lower bound on the temperature of emitting regions on the surface of the neutron star. The typical luminosity of X-ray pulsars is of the order of $L_x \sim 10^{36} \div 10^{37}\,\mathrm{erg\,s^{-1}}$; taking the surface area of two hot spots to be $S = 2ld = 4ad$, the Stefan-Boltzmann law immediately gives

$$T = \left(\frac{L_x}{Sb}\right)^{1/4} \simeq 10^8\,^\circ\mathrm{K} \left(\frac{L_x}{10^{37}\mathrm{erg\,s^{-1}}}\right)^{1/4} \left(\frac{10^5\mathrm{cm}}{a}\right)^{1/4} \cdot \left(\frac{5\times 10^3\mathrm{cm}}{d}\right)^{1/4} . \tag{6}$$

Since the observed spectrum of X-ray pulsars is not that of a black body, the temperature of the atmosphere should in fact exceed the value $10^8\,^\circ$K.

4b) Structure of the Atmosphere

We shall evaluate some characteristic parameters of the atmosphere in the vicinity of hot spots. As a first approximation, we assume a constant temperature over the atmosphere, the density distribution being of the form

$$N_e(z) = N_0 \exp(-z/\mathscr{H}) = (\tau/\sigma_T\mathscr{H}) = 1.2\times 10^{22}\tau(10^8\,^\circ\mathrm{K}/T_e)\mathrm{cm}^{-3} , \tag{7}$$

where $\mathscr{H} = 2kT_eR^2/m_pGM \simeq 1.24\times 10^2(T_e/10^8\,^\circ\mathrm{K})\,\mathrm{cm}$ is the height of the exponential atmosphere (to be more specific, we adopt the mass of the neutron star $M = M_\odot$ and its radius $R = 10^6$cm), and τ is the optical depth for Thomson scattering as before. At this stage, we ignore the pressure gradients due to the emergent light and the infalling material, and this is a good approximation so long as the luminosity is low enough. But if the luminosity is as high as $L_x \sim 10^{35} \div 10^{37}\mathrm{erg\,s^{-1}}$,

both these factors should be taken into account. However, as will be shown in Section 7a, they do not alter the basic qualitative results of this section.

We now compare the free-free opacity with the Thomson scattering opacity. Since the cross-section of either of these processes depends on θ and H in one and the same way [cf. Eqs. (3) and (4)], we may forget for the moment the presence of the magnetic field.

We evaluate the optical depth for free-free absorption at the frequency $h\nu \simeq kT_e$. Using

$$k_{ff} = 3.7\times 10^8 N_e^2 T_e^{-1/2}\nu^{-3}$$
$$= 4.1\times 10^{-23} N_e^2 T_e^{-3.5}(h\nu/kT_e)^{-3}[\mathrm{cm}^{-1}]$$

we find

$$\tau_{ff}(\tau) = \int_z^\infty k_{ff}dz|_{h\nu=kT_e} \simeq 4.5\times 10^{-5}\tau^2(10^8\,^\circ\mathrm{K}/T_e)^{4.5}\,. \quad (8)$$

Thus, the upper layer $\tau \lesssim \tau_0 = 20$, where the main energy of the accreting flow is released, is optically thin with respect to free-free absorption. The efficiency of bremsstrahlung rapidly increases with τ, and when $\tau_{ff}\cdot\tau \sim 1$, i.e. when $\tau \sim 30 > \tau_0$, the local spectrum takes a blackbody form (Illarionov and Sunyaev, 1972a, b; Felten and Rees, 1972). However, this region lies already beyond the layer where the accreting protons deposit their kinetic energy. So the typical photon, emitted in the region $\tau > \tau_0$, diffuses outward through the layer of energy release $\tau \lesssim \tau_0$, increasing its energy there. The total flux of photon number along the vertical axis of the plane-parallel atmosphere is practically constant over the layer $\tau \lesssim \tau_0$. From this we conclude that *one can analyse the diffusion of radiation through the layer* $0 < \tau \lesssim \tau_0$, *idealising the atmosphere as purely scattering one with the source of photons localized at an infinite optical depth.*

4c) Thermal Equilibrium in the Atmosphere

Since the rate of photon creation is negligible in the layer where the accreting protons deposit their kinetic energy, plasma cooling is accompanied by an increase in the mean energy of the photons diffusing outward. Therefore, the primary cooling mechanism will be Compton energy losses by hot electrons when they scatter the low-energy photons. A straightforward calculation also shows the bremsstrahlung to be quite inefficient as a cooling mechanism in the situation being considered here. The analysis of the thermal structure of the atmosphere carried out below is similar to that performed by Zeldovich and Shakura (1969) for the atmosphere of the neutron star without magnetic field.

It was shown in the previous section that the spectrum of the radiation at the optical depth $\tau \gtrsim 30$ is close to that of a black body. Therefore, we can readily estimate the temperature there if the radiative energy density is known. Using the results of our calculations (see Fig. 4 and Section 6) we find the temperature in the layer $\tau \sim 30$ to be $\sim 2\times 10^8\,^\circ$K.

Since the effective optical depth of the layer where the accreting gas deposits its energy is τ_0, the heating rate (per electron) is

$$w^+ = \frac{L_x}{4ad}\frac{\sigma_T}{\tau_0} = Q\frac{\sigma_T}{\tau_0}[\mathrm{erg\,s^{-1}}] \quad (9)$$

where $Q = L_x/S$ is the energy flux per unit surface area. If $3kT_e > \langle h\nu\rangle$, the cooling rate due to Compton scattering is given by

$$w^- \lesssim \frac{8}{15}\frac{\sigma_T \varepsilon_r kT_e}{m_e c} = \frac{16}{15}\sigma_T Q\frac{kT_e}{m_e c^2}\tau[\mathrm{erg\,s^{-1}}] \quad (10)$$

[see Eq. (A5) in Appendix A]. Here we have used the fact that the radiative energy density ε_r increases inwardly and may be taken to be $\simeq 2\tau(Q/c)$. Equating Eqs. (9) and (10), we arrive at the following estimate for the temperature

$$\frac{kT_e}{m_e c^2} \gtrsim \frac{15}{16}\frac{1}{\tau_0\tau}\,; \qquad T_e \gtrsim 3\times 10^8\,^\circ\mathrm{K}/\tau\,. \quad (11)$$

From it one sees that the temperature drops with τ. But as was shown in Section 4a, it cannot become less than $10^8\,^\circ\mathrm{K}(L_x/10^{37}\mathrm{erg\,s^{-1}})^{1/4}$, and consequently the formula (11) is valid only in a thin surface layer $1 \lesssim \tau \lesssim 3$. Thus, the spectrum of the emergent radiation is formed in an atmosphere with varying temperature which grows outward at $\tau \lesssim 3$. The expression (10) is only an upper bound on the cooling rate, since the radiation has an anisotropic angular distribution. The more accurate and much more complicated procedure for calculating $T_e(\tau)$ gives results which are qualitatively the same, and quantitatively close to those obtained above.

5. Radiative Transfer in a Strong Magnetic Field

5a) Qualitative Description of Radiative Transfer at Frequencies $\nu \ll \nu_H$

The radiative transfer in an atmosphere with a strong magnetic field, where the scattering cross-section takes the form (5), has some peculiar features. At any optical depth τ there is a cone of polar angles, $0 \lesssim \theta \lesssim 1/\sqrt{\tau}$, in which the radiation freely escapes from the atmosphere, because the optical depth for scattering within this cone is $\tau_2 = \tau\sin^2\theta/\cos\theta \lesssim 1$ (θ is the angle with respect to the magnetic field which is perpendicular to the plane of the atmosphere). An external observer looking at the atmosphere at an angle θ will pick up the radiation emitted by the layer $\tau \sim \cos\theta/\sin^2\theta$. The intensity of radiative flux detected by such an observer is completely determined by the radiative energy density in this layer[1]).

[1]) The problem under consideration resembles (though cannot be reduced to) the problem of radiative transfer in lines – the photons far in the wings of the line freely escape from the layers opaque to the photons in the centre of the line.

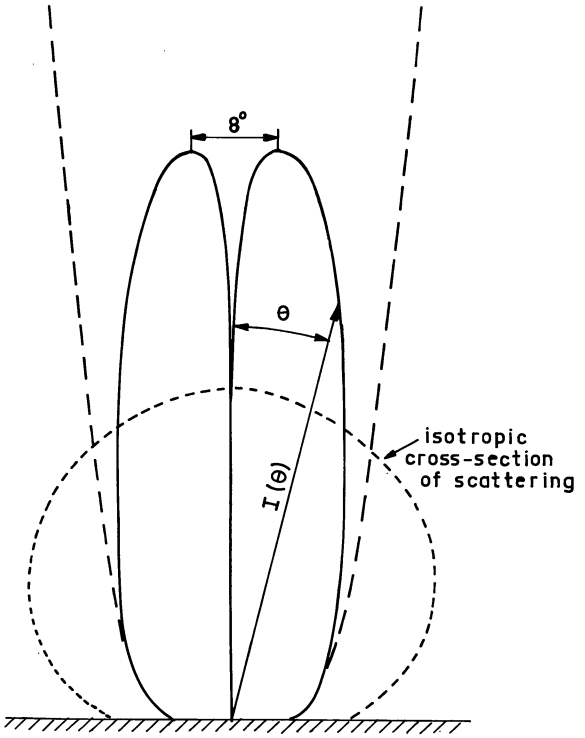

Fig. 3. The indicatrix of the emergent intensity (integrated over the frequency) of purely scattering plane-parallel atmosphere with the cross-section of the form (5). Solid line: the primary sources are distributed exponentially (the rate of energy release $\propto e^{-\tau/20}$). Dashed line: the energy source is localized at the infinite optical depth. Dotted line: the indicatrix of the radiation emerging from the scattering atmosphere with an isotropic scattering cross-section and the energy source at the infinite optical depth

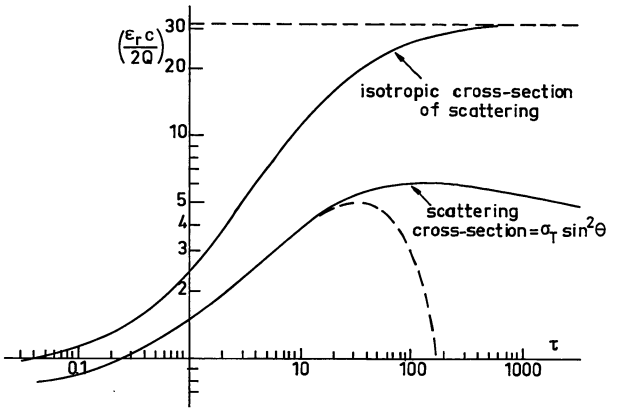

Fig. 4a and b. The run of the radiative energy density ε_r with the optical depth $\tau=\sigma_T\int_z^\infty N_e dz$ for the exponential distribution of primary sources (the rate of energy release $\propto e^{-\tau/20}$) in two limiting cases: (a) the scattering cross-section is isotropic; (b) the scattering cross-section is given by Eq. (5). With a dashed line an approximate behaviour of $\varepsilon_r(\tau)$ is shown for $\nu/\nu_H=10^{-2}$; the "leakage" of energy through the extraordinary wave results in a drop of ε_r at $\tau\sim\nu_H/\nu$. The radiation density ε_r is normalized to $2Q/c$, where Q is the total energy flux emitted by the unit surface area

Since the radiative energy density increases with the optical depth τ (at least for $\tau\lesssim\tau_0$), the intensity of radiation leaving the atmosphere must increase with decreasing angle θ. The angular pattern has the form of a "pencil" beam (see Fig. 3). The angular halfwidth of the beam θ_0 depends on the optical depth τ_0 where the energy release is cut off, $\theta_0\sim 1/\sqrt{\tau_0}\simeq 15^0$.

In an atmosphere with zero magnetic field, the behaviour of the radiative energy density $\varepsilon_r(\tau)$ is governed by the distribution of energy sources over the atmosphere, and also by the stationary diffusion process. In a strong magnetic field, an opportunity arises for photons to come out straight from the large optical depth τ at small angles θ. As a consequence, the function $\varepsilon_r(\tau)$ becomes flatter. The calculated values of $\varepsilon_r(\tau)$ for the exponential distribution ($\propto\exp(-\tau/\tau_0)$) of primary energy sources are plotted in Fig. 4. The strict analysis of the radiative transfer equation in the limit $\nu/\nu_H\to 0$ shows that the radiative energy density $\varepsilon_r(\tau)$ increases with τ for $\tau\lesssim\tau_0$, though not so steeply as in an atmosphere without magnetic field. At $\tau>\tau_0$, where the energy input attenuates exponentially, the curve $\varepsilon_r(\tau)$ flattens, reaches its peak value and then slowly drops due to the "leakage" at small angles θ. We recall that in an atmosphere with an isotropic scattering cross-section, the function $\varepsilon_r(\tau)$ asymptotically approaches a certain constant as $\tau_0<\tau\to\infty$ [see e.g. (Ivanov, 1969)]. For the solution of radiative transfer equation see Appendix B and (Basko, 1975).

If the ratio ν/ν_H is small but finite, an appreciable fraction of radiative energy may leak out by means of the extraordinary wave. As was already mentioned in Section 3, this will result in a more steep drop in $\varepsilon_r(\tau)$ at $\tau>\tau_0$ (dashed line in Fig. 4).

As a result of the drop in radiation density $\varepsilon_r(\tau)$ at $\tau\gg\tau_0$, the angular pattern of the emergent radiation has a narrow "hole" along the axis of "pencil". The angular halfwidth of the hole is quite small ($\lesssim 1°$)[2]). Note that this hole does not disappear even when the emission and the absorption of photons are taken into account.

The formation of a specific beam pattern results from a specific angular dependence of the cross-sections of the elementary processes, and does not depend on the physical character of these processes. For just this reason all of the above arguments hold for the radiative transfer in an atmosphere with free-free and free-bound transitions as the dominant mechanisms of opacity (if one does not consider the dependence of opacity on frequency). The radiation emerging from such an atmosphere will also have a characteristic beam pattern (as in Fig. 3) when strong magnetic field is present.

[2]) The leakage of energy in the extraordinary wave, when $0.1>\nu/\nu_H>0$, may widen this hole to some extent.

5b) Spectrum of Emergent Radiation

The structure of the atmosphere having been analysed and the qualitative description of the radiative transfer having been developed, we can now point out some characteristic spectral features of the emergent radiation. Since the layer where the main part of the energy is released has a negligible optical depth for free-free absorption, the spectrum is defined by the effects of Comptonization. The resulting spectrum is a superposition of comptonized spectra arising at different optical depths.

The form of the comptonized spectrum depends on the value of the parameter $y=\frac{2}{15}(kT_e/m_ec^2)\tau^2$ (for a more detailed discussion see Appendix A). Substituting $T_e\simeq 10^8$ °K and $\tau=\tau_0=20$ we find that $y\sim 1$. The typical photon, emitted in the layer $\tau>\tau_0$, diffuses outwards undergoing a number of scatters and increasing its energy in this way, until it eventually gets into the cone $\theta\lesssim 1/\sqrt{\tau}$ at an optical depth τ and escapes from the atmosphere. The smaller is the final angle θ for the escaping photon, the smaller is the value of the parameter y which corresponds to it.

The theory of Comptonization (Illarionov and Sunyaev, 1974) says that the blackbody spectrum and that of a bremsstrahlung flatten considerably when the parameter y is as small as $0.1\lesssim y\lesssim 1$. Thus, the resulting spectrum should be rather flat up to the photon energies $h\nu\sim(1\div 3)kT_e$ and then drop exponentially.

i) The Case $kT_e\ll h\nu_H$. Since the flux of the photon number is nearly constant over the region of energy release while the energy flux drops exponentially ($\propto\exp(-\tau/\tau_0)$), low energy photons $h\nu<kT_e$ prevail in the radiative energy density in deep layers. As a consequence, the low energy photons $h\nu<kT_e$ will form a narrower beam [and the high energy photons ($h\nu>kT_e$), respectively – a broader one] than the total energy beam depicted in Fig. 3 with a solid line. The other reason for the beam be less pronounced at high frequencies is the dependence of the scattering cross-section (3) on the ratio ν/ν_H: at high frequencies one cannot "see" extremely deep layers $\tau>(\nu_H/\nu)^2$.

(ii) The Case $kT_e\gtrsim h\nu_H$; *Emission Gyroline.* To analyse the angular distribution of the emergent radiation in this case, one should take into account the dependence of the scattering cross-section on frequency. At $\nu\ll\nu_H$ a narrow beam is formed as in the previous case; at $\nu\lesssim\nu_H$ the effect of beaming becomes less pronounced, and at $\nu>\nu_H$ it practically disappears.

On the frequency $\nu=\nu_H$ a powerful gyroline should stand out against the continuum. Really, the optical depth with respect to free-free absorption in the atmosphere is much smaller than that for Thomson scattering. The intensity of radiation leaving such an atmosphere is always lower than the blackbody value (Shakura, 1972; Felten and Rees, 1972; Illarionov and Sunyaev, 1972b). At the same time, the optical depth for cyclotron absorption is exceedingly large in the case of interest here. Then the intensity in the line must reach the blackbody value, i.e. must exceed significantly the continuum level. This gyroline must be wide enough, $\Delta\nu/\nu\gtrsim 3^{-1/2}(2kT_e/m_ec^2)^{1/2}\sim 0.1$.

Note that the X-ray lines due to the atomic transitions should in fact be very weak, since in atmosphere with $T_e>10^8$ °K all of the most abundant elements are completely ionized. To discover lines in the spectra of X-ray sources, it would be most promising perhaps to search for gyrolines and K_α-lines of iron and other heavy elements, the latter arising from the atmosphere of the normal X-ray binary component illuminated by the hard X-ray continuum (Basko *et al.*, 1974).

5c) Polarization

The beamed radiation is highly polarised, and both the linear and the circular polarization should be observed. The polarization for the model considered here is discussed in detail by Gnedin and Sunyaev (1974).

6. Results of Numerical Calculations

The equation of transfer, the method of solution of which is outlined in Appendix B, describes adequately radiative transfer in an atmosphere with a strong magnetic field only when the condition $\nu\ll\nu_H$ holds over the whole frequency range, i.e. in the limit $kT_e\ll h\nu_H$. If the primary sources are distributed exponentially ($\propto\exp(-\tau/\tau_0)$), the emergent radiative energy flux per unit solid angle $I(0,\cos\theta)$ can be expressed in terms of Chandrasekhar's H-function $H(x)$ [see Eq. (B12)]. The form of the angular pattern depends on the parameter τ_0 only. The effective halfwidth of the pencil beam is $\theta_0\sim 1/\sqrt{\tau_0}$. The function $H(x)$ was calculated numerically by one of the authors and the results are tabulated in (Basko, 1975). The resulting beam pattern for $\tau_0=20$ is presented in Fig. 3 with a solid line. The beam has a narrow hole in its centre which has already been discussed in Section 5a.

Figure 5 illustrates the pulse profile as detected by an observer in the spin plane of the neutron star, the magnetic dipole axis of which is perpendicular to the spin axis. The energy flux detected by the distant observer (solid line) is equal to the emergent intensity $I(0,\cos\theta)$ (dashed line) multiplied by $\cos\theta$. The factor $\cos\theta$ arises from the fact that the radiation emerges from two plane areas small compared to the surface of the neutron star. The pulse is rather narrow and high, but in spite of this fact more than half of the total energy leaves the surface at the angles $\theta>30°$ because the corresponding solid angle is large. The observed pulse shape (Holt *et al.*, 1974) is somewhat broader than that illustrated in Fig. 5.

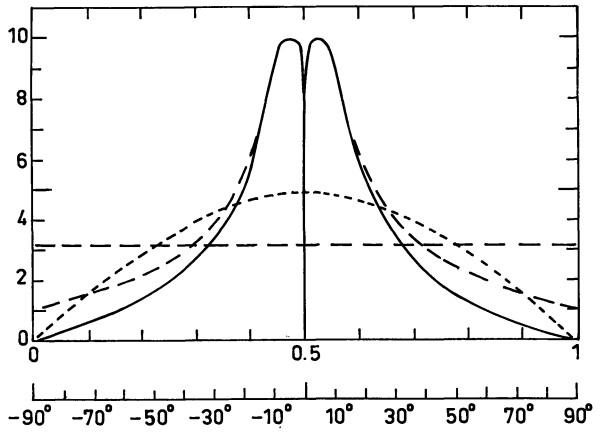

Fig. 5. The X-ray pulse profile as registered by the distant observer in the equatorial plane of the neutron star when its spin axis is perpendicular to the magnetic dipole axis. The abscissae are the pulse phases normalized to the half of the revolution of the neutron star. Solid line: the energy flux (in arbitrary units) as detected by distant observer. It is equal to the emergent intensity (dashed line) integrated over the frequency and multiplied by $\cos\theta$. For comparison the dashed straight line and the dotted sinusoid are plotted, the areas under which are equal to the area under the solid curve. Recall that an isotropically radiating plane hot spot gives a sinusoidal pulse profile

In Section 4b it was shown that the photon-number flux is practically constant over the upper atmospheric layer $\tau \lesssim \tau_0$ considered here. If one assumes that the source of photons is localized infinitely deep in the atmosphere, then the emergent photon-number intensity will be given by formula (B10). Its angular dependence is shown in Fig. 3 with a dashed line. To obtain the actual photon-number beam pattern, one should "cut off" the beam of Fig. 3 at the angles $\theta \lesssim 1/\sqrt{\tau_f}$. Here $\tau=\tau_f$ is the optical depth of the layer where either emission and absorption of photons, or leakage by the extraordinary wave, become important.

7. Limits on the Luminosity of Accreting X-ray Pulsars

a) Radiative Pressure

The scheme developed above for the reprocessing of the accreting gas energy breaks down when the emergent radiation field substantially distorts the accretion pattern, i.e. when the infalling gas loses a substantial fraction of its kinetic energy by the interaction with the emergent radiation field. The pressure of the emergent radiation may be represented as the effective deceleration

$$g_{\rm eff}(z)=2\pi(\sigma_T/m_p c)\int_{\hat\mu(z)}^{1} I(0,\mu)\,\mu(1-\mu^2)\,d\mu\,. \qquad (12)$$

Here $\hat\mu(z)=[1+(d/2z)^2]^{-1/2}$, z is the height above the stellar surface, d is the width of the accretion column. The factor $(1-\mu^2)=\sin^2\theta$ in the integrand allows for the angular dependence of the scattering cross-section (3) in a strong magnetic field. The numerical evaluation of the integral in (12) at $z=0$ for $\tau_0=20$ gives

$$g_{\rm eff}(0)=\tfrac{1}{3}(\sigma_T/m_p)Q/c\,; \qquad (13)$$

thus, an extremely strong magnetic field reduces the light pressure at the surface to one third of its value in the absence of field. (Q is the radiative energy flux per unit surface area.) If $z \gg d$, one can substitute $\hat\mu(z)=1-\frac{1}{2}(d/2z)^2$ into (12) and find that

$$g_{\rm eff}(z)\propto(d/z)^4\,. \qquad (14)$$

In other words, the effect of emergent radiation on the accreting material is negligible at $z>d$, and light pressure decelerates the infalling matter effectively in the layer $0<z\lesssim d$.

One can ignore the influence of radiation on the accreting matter so long as $g_{\rm eff}(0)d/c \ll \frac{1}{2}c$ ($v\simeq\frac{1}{2}c$ is the flow velocity, and d/c characterizes the time for which decelerating force acts). This condition imposes a restriction on the radiative energy flux

$$Q \ll \tfrac{3}{2}(m_p/\sigma_T)c^3/d$$

and, consequently, on the total luminosity of the X-ray pulsar. Taking the cross-length of either of two accretion columns on magnetic poles (see Fig. 2) to be $l=2a=2\times10^5$cm, we thus obtain

$$L_x=2Qld \ll 3(m_p/\sigma_T)\,lc^3\simeq 4\times10^{37}(a/10^5{\rm cm})\,{\rm erg\,s^{-1}}. \qquad (15)$$

Note that this estimate does not depend on the value of d, and, therefore, neither on the form of the cross-section of the accreting columns. The luminosity may be expressed in terms of the gas density N_e; having done this, one can rewrite (15) in the form:

$$\tau_t=\sigma_T N_e d \ll 24\,,$$

where τ_t is the Thomson optical depth across the accretion column.

If the pulsar luminosity approaches the upper limit, $L_x\sim10^{37}{\rm erg\,s^{-1}}$, then for the adopted geometry of accretion the light pressure (13) may exceed the gravity acceleration $g=GM/R^2$ by two orders of magnitude; or, equivalently, the radiation flux per unit surface area may exceed by two orders of magnitude the critical Eddington value. In such a situation, the light pressure and the momentum transfer by deceleration of the accreting gas must be included in the balance of forces acting on the atmosphere.

The infalling protons exert a downward force equal to (per nucleon of the atmosphere at rest)

$$(2Q/v)\sigma_{pp}=(4Q/c)\sigma_{pp}\,,$$

where $\sigma_{pp}\simeq3\times10^{-26}{\rm cm}^2$ is the cross-section of strong interaction[3]), and $Q=\varrho v^3/2$ is the kinetic energy flux

[3]) In nuclear collisions the accreting protons are forced to leave the magnetic force lines. Once deflected they rapidly lose their energy by Coulomb collisions with electrons through transverse momentum transfer. In the course of this rapid thermalization the protons give up their initial downward momentum to the ambient plasma.

of accreting protons equal to the emergent radiative flux. The ratio of this force to the upward pressure of light (13) is $12\sigma_{pp}/\sigma_T \simeq 0.5$. Hence, the light pressure pushes out material from the atmosphere along the magnetic field lines. However, the maximum height at which this material can be pushed out is of the same order of magnitudes as d, since the light pressure, as one sees from (14), rapidly drops at $z > d$. Recalling that $d > \mathscr{H}$, we conclude that the atmosphere in this case will be still more rarefied than the estimates of Section 4b show it to be, and Compton scattering will be still more dominant in the opacity.

7b) Distortion of Beam Pattern

The X-ray emission of the rotating neutron star will pulsate properly only when the beam pattern distortion due to interaction with the infalling gas is small enough. The effective [with the dependence $\sigma(\theta)$ taken into account] optical depth for the photon leaving the atmosphere from the middle of the accretion column is

$$\tau_2 = \sigma_T \sin^2\theta N_e (d/2\sin\theta) = \tfrac{1}{2}\sigma_T N_e d \sin\theta = \tfrac{1}{2}\tau_t \sin\theta .$$

For $\theta = 30°$ it is 4 times less than the optical depth across the accretion column τ_t. This imposes a restriction $\tau_t < 4$, or $L_x < 7 \times 10^{36}\,\mathrm{erg\,s^{-1}}$.
Note that the beaming mechanisms proposed so far (Gnedin and Sunyaev, 1973a; Bisnovatyi-Kogan, 1973) fail to work under somewhat harder restriction $\tau_t < 1$. It is very likely that this result is of a general character, and that *all accreting X-ray pulsars must have luminosities* $L_x \lesssim 10^{37}\,\mathrm{erg\,s^{-1}}$. On the other hand, there is a lower bound on the luminosity of an accreting rotating magnetic neutron star; if the rate of mass transfer in the binary is low enough, the rotating magnetic dipole throws away the ambient gas and thereby inhibits accretion (Illarionov and Sunyaev, 1975). The existence of these lower and upper bounds on the luminosity may well account for such a miserable number of accreting X-ray pulsars (only two of them!) in the Galaxy.

7c) Comparison with Observational Data

The X-ray pulsar Her X-1 is at the distance $D \simeq 4$ kpc (Basko and Sunyaev, 1973). According to the X-ray data (McClintock *et al.*, 1974) its luminosity per unit solid angle averaged over pulsational period is $\langle \mathscr{L}_x \rangle \simeq 9 \times 10^{35}$erg/s sterad. In the case of a pencil beam pattern one has

$$\langle \mathscr{L}_x \rangle = \mathscr{L}_x (2\theta_0/\pi) ,$$

where θ_0 is the angular halfwidth of the beam, and $\mathscr{L}_x$ is the luminosity per unit solid angle at $0 < \theta < \theta_0$. The observations (Holt *et al.*, 1974) show that $2\theta_0/\pi \simeq 0.4$. The total luminosity of the X-ray pulsar Her X-1 is

$$L_x = 2\mathscr{L}_x 2\pi(1-\cos\theta_0) = 2\langle \mathscr{L}_x \rangle (\pi^2/\theta_0)(1-\cos\theta_0)$$
$$\simeq 5 \times 10^{36}\,\mathrm{erg\,s^{-1}} .$$

However, as was mentioned in the previous section, in our beaming model about the half of the total energy may leave the atmosphere at angles $\theta > 30°$, though the flux detected by a properly oriented observer will be small. Allowing for this fact we arrive at the following estimate for the luminosity of Her X-1

$$L_x = (0.5 \div 1) \times 10^{37}\,\mathrm{erg\,s^{-1}} ,$$

which is consistent with the results obtained above.
The spectrum of another X-ray pulsar Cen X-3 is softer than that of Her X-1. Its distance is evaluated to be $D \sim 7$ kpc (Mauder, 1974). Assuming that $2\theta_0/\pi \simeq 0.4$ in this case too and using the UHURU data, we find the luminosity of Cen X-3 to be $L_x \simeq 7 \times 10^{36} (D/7\,\mathrm{kpc})^2\,\mathrm{erg\ s^{-1}}$. For $D \lesssim 7$ kpc this estimate is also consistent with the above argument.

8. Optical Pulsations from Magnetic White Dwarfs

The above model for X-ray beaming can be also applied to optical radiation of white dwarfs with a strong magnetic field $H \gtrsim 10^9$ Gauss such that the range $\nu < \nu_H$ turns out to be in the optical (see Section 5a above). The energy release by accretion in this case will be also confined to small spots at the magnetic poles. For the emergent optical radiation to be beamed, it is required also that the main energy release in the atmosphere occur at least at the optical depth $\tau \gtrsim 5 \div 10$.
However, the bright spots at the magnetic poles may exist even when the luminosity is due to an energy flux from inner regions of white dwarf. In this case, the increase in the surface brightness towards the magnetic poles results from the reduction of opacity along field lines (Smoluchowski, 1972).
The beamed optical radiation should be polarized (Gnedin and Sunyaev, 1974). It is possible that in the framework of the above model one can satisfactorily explain the weak optical pulsations and the variable polarization in the wellknown system DQ Her.

Acknowledgements. The authors wish to thank Yu. N. Gnedin, G. G. Pavlov and Ya. B. Zeldovich for many helpful discussions.

Appendix A

Comptonization of Radiation in a Strong Magnetic Field

In a non-magnetized plasma the scattering of low-energy photons by hot electrons leads to an increase in the mean photon energy and to a deformation of

spectral shape of the radiation field (Kompaneets, 1956; Illarionov and Sunyaev, 1974). It is shown below that a strong magnetic field, $h\nu_H > kT_e$, reduces the rate of Comptonization by the factor of 7.5.

Consider an electron moving through the isotropic radiation field of energy density ε_r and of arbitrary spectral shape. We evaluate the decelerating force exerted on this electron. For this we pass to its rest frame. In this frame of reference, the radiation field will be anisotropic because of the Doppler shift. The radiative energy flux per unit surface area per unit solid angle takes the form

$$I(\theta)=\frac{\varepsilon_r c}{4\pi}\left(1-\frac{v^2}{c^2}\right)^2\left(1+\frac{v}{c}\cos\theta\right)^{-4}, \tag{A1}$$

where $\boldsymbol{v}$ is the electron velocity, and θ is the angle that $\boldsymbol{v}$ makes with the direction of photon propogation. The force of the light pressure exerted on the electron along $\boldsymbol{v}$ is given by

$$f=\sigma_T/c\int I(\theta)\cos\theta\,\mathrm{d}\Omega\,, \tag{A2}$$

where σ_T is the Thomson cross-section, $d\Omega$ the element of solid angle. The factor $\cos\theta$ allows for that projection of momentum transfer which is of interest here. In deriving (A2) the fact was also used that the total momentum carried away by the scattered radiation field vanishes in the electron rest frame. The expression (A2) is purely classical: it takes no account of the quantum effect of frequency shift by scattering. Substituting (A1) into (A2) we find that to first order in v/c

$$f=\frac{\sigma_T\varepsilon_r}{2}\int_{-1}^{+1}\left(1-4\frac{v}{c}\cos\theta\right)\cos\theta d\cos\theta=-\frac{4}{3}\sigma_T\varepsilon_r\frac{v}{c}, \tag{A3}$$

which is a well-known result in classical electrodynamics (Landau and Lifshitz, 1967).

In an analogous way, one easily finds the decelerating force exerted on the electron moving through the radiation field along the axis of a strong magnetic field

$$f=\frac{\sigma_T\varepsilon_r}{2}\int_{-1}^{+1}\left(1-4\frac{v}{c}\cos\theta\right)\cos\theta\sin^2\theta d\cos\theta$$
$$=-\frac{8}{15}\sigma_T\varepsilon_r\frac{v}{c}. \tag{A4}$$

It turns out to be 2.5 times less than the corresponding force (A3) in the absence of a magnetic field. In deriving (A4) we used the formula (3) for the scattering cross-section in the limit $v/\nu_H\to 0$.

From (A3) and (A4) one can easily obtain the rate of energy exchange between the plasma and the radiation field:

$$\frac{d\varepsilon_r}{dt}=-N_e\frac{d}{dt}\left(\frac{m_e v^2}{2}\right)=-N_e f v$$
$$=\begin{cases}\frac{8}{3}\,\frac{\sigma_T N_e\varepsilon_r}{m_e c}\,\frac{m_e v^2}{2}, & v\gg v_H\,;\\ \frac{16}{15}\,\frac{\sigma_T N_e\varepsilon_r}{m_e c}\,\frac{m_e v^2}{2}, & v\ll v_H\,.\end{cases} \tag{A5}$$

In the non-magnetized plasma $\langle m_e v^2/2\rangle=\frac{3}{2}kT_e$, and the solution of (A5) is $\varepsilon_r=\varepsilon_r^{(0)}e^{4y}$. Here the Comptonization parameter y is given by $(kT_e/m_e c^2)\sigma_T N_e ct$ in the case of an infinite homogeneous medium, and by $y=(kT_e/m_e c^2)\tau_T^2$ in the case of the atmosphere (or a source) of the optical depth τ_T (Illarionov and Sunyaev, 1972a). In a strong magnetic field $h\nu_H > kT_e$ the electron motion is one-dimensional and $\langle m_e v^2/2\rangle=\frac{1}{2}kT_e$. Then from (A5) one immediately gets $y=\frac{2}{15}(kT_e/m_e c^2)\sigma_T N_e ct$, and $y=\frac{2}{15}(kT_e/m_e c^2)\tau_T^2$ respectively. Thus, the strong magnetic field reduces the value of parameter y by the factor of 7.5.

In the other interesting case $v > \nu_H > \Delta\nu_D = (2kT_e/m_e c^2)^{1/2}\cdot\nu$ the exact calculations confirm the conclusion made by Gnedin and Sunyaev (1973b, c): the magnetic field does not affect the rate of Comptonization; one third of the energy transfer in this case is due to Doppler broadening, and two thirds – due to the basic frequency satellites arising from scattering.

Appendix B

Solution of the Equation of Transfer

Let the z-axis be perpendicular to the plane-parallel atmosphere and directed outward, and let $\theta=\arccos\mu$ be the polar angle as measured from this axis. Then the equation of transfer for a cross-section of the form (5) becomes (the atmosphere is assumed to be purely scattering)

$$\mu\frac{\partial I(z,\mu)}{\partial z}=-\sigma_T(1-\mu^2)N_e I(z,\mu)$$
$$+\sigma_T(1-\mu^2)N_e\tfrac{3}{4}\int_{-1}^{+1}(1-\mu'^2)\,I(z,\mu')\,d\mu' \tag{B1}$$
$$+\sigma_T(1-\mu^2)N_e S^*(z)\,.$$

Here $I(z,\mu)$ is the intensity of radiation integrated over the frequency. The adopted angular dependence of the source term $\sigma_T(1-\mu^2)N_e S^*(z)$ results from the fact that Compton scattering is the dominant mechanism of plasma cooling (see Section 4c).

Introducing a new independent variable $\tau=\sigma_T\int_z^\infty N_e dz$ we rewrite (B1) as follows:

$$\frac{\mu}{1-\mu^2}\frac{\partial I(\tau,\mu)}{\partial\tau}=I(\tau,\mu)-\tfrac{3}{4}\int_{-1}^{+1}(1-\mu'^2)\,I(\tau,\mu')\,d\mu'-S^*(\tau)\,. \tag{B2}$$

When multiplied by $2(1-\mu^2)$ and integrated over μ, Eq. (B2) gives

$$\frac{dF(\tau)}{d\tau} \equiv F'(\tau) = -\tfrac{8}{3}S^*(\tau),$$

where $\pi F(\tau) = 2\pi\int_{-1}^{+1}\mu I(\tau,\mu)d\mu$ is the radiative energy flux along z-axis. We write $L(\tau) = \tfrac{3}{4}\int_{-1}^{+1}(1-\mu^2)I(\tau,\mu)d\mu$ and introduce the source function

$$S(\tau) \equiv L(\tau) + S^*(\tau) = L(\tau) - \tfrac{3}{8}F'(\tau). \tag{B3}$$

One can easily show that the source function satisfies the integral equation

$$S(\tau) = \tfrac{1}{2}\int_0^\infty R(|\tau-t|)\,S(t)dt - \tfrac{3}{8}F'(\tau), \tag{B4}$$

where the kernel $R(\tau)$ takes the form

$$R(\tau) = \tfrac{3}{2}\int_0^1 \frac{(1-\mu^2)^2}{\mu}\exp[-\tau(1-\mu^2)/\mu]d\mu. \tag{B5}$$

With the aid of a technique developed for line-transfer problems [for a more detailed discussion see (Ivanov, 1969)] the solution of Eq. (B4) reduces to the calculation of the resolvant function $\Phi(\tau)$ which satisfies the following integral equation

$$\Phi(\tau) = \tfrac{1}{2}\int_0^\infty R(|\tau-t|)\,\Phi(t)dt + \tfrac{1}{2}R(\tau). \tag{B6}$$

The Laplace transform of $\Phi(\tau)$ leads to Chandrasekhar's well known H-function

$$H(x) = 1 + \int_0^\infty \Phi(t)e^{-t/x}dt. \tag{B7}$$

In the interval $0 \leqslant x < +\infty$, the H-function increases monotonically from $H(0)=1$ up to $H(+\infty)=+\infty$. One can show also that $\lim_{x\to\infty} H(x)/x = 0$, which leads to $\lim_{\tau\to\infty}\Phi(\tau) = 0$. Such a behaviour of $\Phi(\tau)$ at infinity results in the presence of a narrow "hole" in the beam pattern (B12). The numerical calculations (Basko, 1975) show that within the interval $5 \lesssim x \lesssim 10^4$ the function $H(x)$ can be approximated to an accuracy of $\sim 3\%$ by the expression

$$H(x) = 1.62x/(\ln x)^{0.645} \tag{B8}$$

Of particular interest are the two simplest distributions of primary sources $S^*(\tau) = -\tfrac{3}{8}F'(\tau)$:

a) $F'(\tau) = 0$, Constant Radiative Energy Flux.

In this case Eq. (B4) becomes homogeneous. Differentiating it with respect to τ and comparing the result with (B6), we conclude that $S'(\tau) = S(0)\Phi(\tau)$ and

$$S(\tau) = L(\tau) = S(0)\,[1 + \int_0^\tau \Phi(t)dt]. \tag{B9}$$

The emergent intensity is given by

$$I(0,\mu) = S(0)\,H(\mu/1-\mu^2). \tag{B10}$$

b) $F(\tau) = (Q/\pi)\exp(-\tau/\tau_0)$, Exponential Distribution of Primary Sources.

One can show that in this case

$$S(\tau) = \tfrac{3}{8}(Q/\pi)\,(H(\tau_0)/\tau_0)\,\{e^{-\tau/\tau_0} + \int_0^\tau \Phi(t)\exp[-(\tau-t)/\tau_0]\,dt\}. \tag{B11}$$

The emergent intensity turns out to be

$$I(0,\mu) = \frac{3}{8}\frac{Q}{\pi}\frac{H(\tau_0)H[\mu/(1-\mu^2)]}{\mu/(1-\mu^2)+\tau_0}. \tag{B12}$$

References

Baan, W. A., Treves, A. 1973, *Astron. & Astrophys.* **22**, 421
Basko, M. M. 1975, *Astrofizika* (in press)
Basko, M. M., Sunyaev, R. A. 1973, *Astrophys. Space Sci.* **23**, 117
Basko, M. M., Sunyaev, R. A., Titarchuk, L. G. 1974, *Astron. & Astrophys.* **31**, 249
Basko, M. M., Sunyaev, R. A. 1975, JETP **68**, 105
Bisnovatyi-Kogan, G. S. 1973, *Astron. Zh.* **50**, 902
Canuto, V., Lodenquai, J., Ruderman, M. 1971, *Pys. Rev. D.* **3**, 2303
Daishido, T. 1975, *Publ. Astron. Soc. Japan* **27**, 181
Davidson, K., Ostriker, J. P. 1973, *Astrophys. J.* **179**, 585
Felten, J. E., Rees, M. J. 1972, *Astron. & Astrophys.* **17**, 226
Fermi, E. 1950, Nuclear Physics, Chicago
Ginzburg, V. L., Ruhadze, A. A. 1970, Waves in Magnetized Plasmas, "Nauka", Moscow
Gnedin, Yu. N., Sunyaev, R. A. 1973a, *Astron. & Astrophys.* **25**, 233
Gnedin, Yu. N., Sunyaev, R. A. 1973b, JETP **65**, 102
Gnedin, Yu. N., Sunyaev, R. A. 1973c, *Monthly Notices Roy. Astron. Soc.* **162**, 53
Gnedin, Yu. N., Sunyaev, R. A. 1974, *Astron. & Astrophys.* **36**, 379
Holt, S. S., Boldt, E. A., Rothschild, R. E., Saba, J. L. R., Serlemitsos, P. J. 1974, *Astrophys. J.* **190**, L 109
Illarionov, A. F., Sunyaev, R. A. 1972a, *Astron. Zh.* **49**, 58
Illarionov, A. F., Sunyaev, R. A. 1972b, *Astrophys. Space Sci.* **19**, 61
Illarionov, A. F., Sunyaev, R. A. 1974, *Astron. Zh.* **51**, 698
Illarionov, A. F., Sunyaev, R. A. 1975, *Astron. & Astrophys.* **39**, 185
Ivanov, V. V. 1969, Radiative Transfer and Celestial Body Spectra, "Nauka", Moscow
Kompaneets, A. S. 1956, JETP **31**, 876
Lamb, F. K., Pethick, C. J., Pines, D. 1973, *Astrophys. J.* **184**, 271
Landau, L. D. 1937, JETP **7**, 203
Landau, L. D., Lifshits, E. M. 1967, Field Theory, "Nauka", 5-th Edd., Moscow
Lodenquai, J., Canuto, V., Ruderman, M., Tsuruta, S. 1974, *Astrophys. J.* **190**, 141
Mauder, H. 1974, preprint; *Astrophys. J.* (in press)
McClintock, J. E., Clark, G. W., Lewin, W. H. G., Schnopper, H. W., Canizares, C. R., Sprott, G. F. 1974, *Astrophys. J.* **188**, 159
Pringle, J. E., Rees, M. J. 1972, *Astron. & Astrophys.* **21**, 1
Smoluchowski, R. 1972, *Nature Phys. Sci.* **240**, 54
Shakura, N. I. 1972, *Astron. Zh.* **49**, 652
Ventura, J. 1973, *Phys. Rev. A.* **8**, 3021
Zeldovich, Ya. B., Shakura, N. I. 1969, *Astron. Zh.* **46**, 225

M. M. Basko
R. A. Sunyaev
Space Research Institute
Academy of Sciences of the USSR
Profsoyuznaja 88
Moscow 117810, USSR